Exploring the role of palm concavity and adaptability in soft synergistic robotic hands

P. Capsi-Morales[1,2], G. Grioli[1], C. Piazza[2], A. Bicchi[1,2] and M. G. Catalano[1].
RAL version

***Abstract*—Robotic hand engineers usually focus on finger capabilities, often disregarding the palm contribution. Inspired by human anatomy, this paper explores the advantages of including a flexible concave palm into the design of a robotic hand actuated by soft synergies. We analyse how the inclusion of an articulated palm improves finger workspace and manipulability. We propose a mechanical design of a modular palm with two elastic rolling-contact palmar joints, that can be integrated on the Pisa/IIT SoftHand, without introducing additional motors. With this prototype, we evaluate experimentally the grasping capabilities of a robotic palm. We compare its performance to that of the same robotic hand with the palm fixed, and to that of a human hand. To assess the effective grasp quality achieved by the three systems, we measure the contact area using paint-transfer patterns in different grasping actions. Preliminary grasping experiments show a closer resemblance of the soft-palm robotic hand to the human hand. Results evidence a higher adaptive capability and a larger involvement of all fingers in grasping.**

***Index Terms*—Grasping, Multifingered Hands, Soft Robot Applications, Underactuated Robots.**

I. INTRODUCTION

PREHENSION is a very developed function of the human hand, an organ capable to adapt to an object-based both on its shape and the intended use [1]. Compared to other animal hands, one of the most apparent differences is its superior quality of opposition, that reflects in the wide range of purpose actions capable to execute. Many studies focus on finger kinematics and hand-arm orientation to characterize reaching and grasping motions (see [2] for review). Nonetheless, while fingers play an important role, also the palmar concavity determines the ultimate hand posture and gives a fundamental contribution to provide an adequate and stable grasp [1].

Manuscript received: February 24, 2020; Revised April 13, 2020; Accepted June 6, 2020.

This paper was recommended for publication by Hong Liu upon evaluation of the Associate Editor and Reviewers' comments. *This research has received funding from the European Union's Horizon 2020 Research, Innovation Programme under Grant Agreement No.688857 (SoftPro), No. 871352 (ReconCycle) and ERC programme under the Grant Agreement No.810346 (Natural Bionics). The content of this publication is the sole responsibility of the authors. The European Commission or its services cannot be held responsible for any use that may be made of the information it contains.

[1]Soft Robotics for Human Cooperation and Rehabilitation, Istituto Italiano di Tecnologia, Genoa, Italy

[2]Centro di Ricerca "E. Piaggio", Universita di Pisa, Largo L. Lazzarino, 1, 56126 Pisa, Italy. Correspond to: patri.capsi@gmail.com

Digital Object Identifier (DOI): see top of this page.

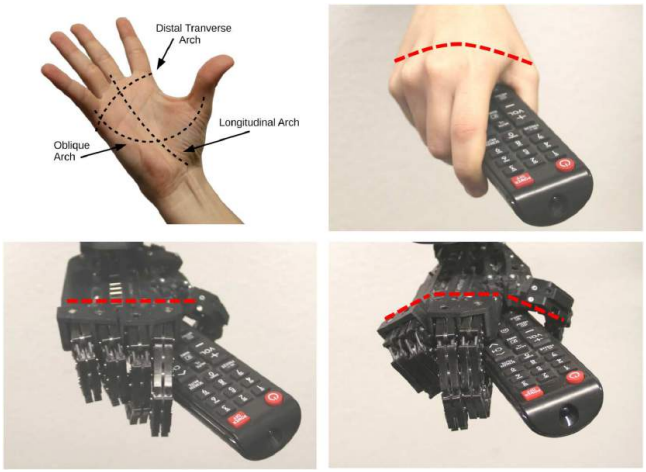

Figure 1. Palm arches are defined in the top left corner [1]. Top right corner shows a human hand grasping a remote control, highlighting the contribution of palm concavity. Bottom left corner presents a robotic hand performing the same grasping action without palm contribution. Finally, a new version of the Pisa/IIT SoftHand [3] with a modular palm actuated together with fingers closure is presented in the bottom right corner. The red dashed lines emphasize the similarities in palm contribution between the human hand and the proposed system.

Anatomical studies identified features that facilitate prehension, such as the capability of the index finger to rotate towards the fifth finger, and the reciprocal rotation of the fifth finger towards the index and the thumb [4]. The thenar muscles, responsible for the thumb movement, allow for an opposable thumb. However, the hypothenar muscles, that intersects the base of the hand at carpal bones level to the base of the fifth finger, have also a substantial contribution in preshaping and contact shaping. These features enable the accommodation of large stresses associated with opposition, and result in sophisticated manipulation capabilities.

In robotics, many highly anthropomorphic hand prototypes were designed over the last century [5]. Their grasping capabilities are usually engineered through complex finger structures and sophisticate actuation mechanisms, but relatively little research focuses on the inclusion of the palm. Some systems approximate the palm concavity through a rigid curved surface, as the DLR Hand II [6], while another explores an extremely biomimetic approach [7]. Very few examples propose active palms at the cost of requiring additional actuators like [8], [9] and [10]. More recently, through the introduction of soft robotic technologies, the importance of flexible palms has been investigated in hands,

as in [11] or [12].

In this paper, we study the contribution of the palm concavity and its deformation to the motions of a robotic hand. We study how this feature affects the mobility and workspace of fingertips. Encouraging results led us to the inclusion of an articulated palm in the design of an existing soft robotic hand (the Pisa/IIT SoftHand [3]). We propose a two degrees of freedom deformable palm, able to emulate the motions of the thenar and hypothenar muscles. Most noticeably, we adjust the synergetic under-actuation mechanism of the hand to actuate also the palm motions, with the advantage of not introducing additional motors in the system. Finally, we validate its feasibility and the effect of palm motions integration in active grasping, compared to a system where palm motions are inhibited and to a human hand. We explore the quality of the achieved grasps, measured in terms of contact area, and the adaptive capability of the proposed system in more functional grasping actions.

The paper is organized as follows: Section II presents the role of the palm in manipulation, Section III shows an analysis of kinematics and manipulability of robotic hands with modular palms. It also presents a grasp comparison between a hand with the palm included or not in its closure synergy in simulation. Section IV describes the mechanical design proposed and its implementation. Section V exposes the experimental validation and we discuss the results in Section VI. Section VII concludes this work and proposes future directions.

II. BACKGROUND

The complex architecture of the human hand is difficult to translate in an artificial system. Consequently, some of its salient features are often sacrificed during the design process, to favour simplicity despite introducing discrepancies between the artificial prototype and its biological inspiration.

A common simplification approach consists in concentrating on the fingers and their dexterity, while neglecting the palm concavity. However, the palm constitutes the socket grounding for the thumb and the rest of the fingers, and the palm motion has a crucial role in the definition of the hand configuration, especially when grasping. Indeed, during pregrasping and grasping phases, the palmar and dorsal surfaces of the human hand change according to the shape of the target to increase the contact surface.

In traditional anatomical definitions [13], the hollow cavity of the palm is described by three arches that run in different directions (see top left in Fig. 1): *the Distal transverse arch:* a concave curvature at the metacarpal heads of the index, middle, ring and fifth finger, *the Longitudinal arch:* a carpometacarpo-phalangeal arch that extends from the wrist to the base of the middle or index fingers, and *the Oblique arch:* a diagonal concavity formed by the thenar eminence and the thumb with the rest fingers.

A more recent work [1] analyses the palm kinematically by describing it with three planes, and by measuring the thenar and hypothenar angles. These are the two angles formed by the thumb base (the thenar eminence) and the fifth finger plane (the hypothenar eminence) with respect to the central palm plane. The study found a significant influence of the overall thenar and hypothenar angles in power-grasping tasks. In particular, while the thenar contribution was more significant in transport shaping, hypothenar contribution was evident in pregrasping and major in contact shaping, i.e. when the hand established contact with the object. This finding was interesting since previous studies [14] tended to consider important the thenar movement alone.

Factors such as object size, location and intended use influence hand shape modulation, and different palmar shape and contribution can be experienced (e.g. when performing precision grasp, where more finger dexterity is involved). Therefore, object-dependent classifications have been proposed to sort human prehensile patterns (e.g. [15], [16]). Napier [14] expresses a different viewpoint indicating that patterns should not be determined mainly by object shape, but by the action purpose. In [17], the authors specify fundamental patterns without regard to any specific activity or any specific group of objects. Pattern characteristics are determined by the position of the fingers and by the existent contact areas, which give a supplemental value to identify them. Accordingly, [18] classified 14 patterns under 4 big categories, where power grip is the only one where the palm makes direct contact with the object.

In literature, especially in ergonomics, the study of contact areas and pressure distribution, e.g. during hand-handle interactions [19], have been widely investigated. Another example is [20], a study on the forces exchanged between hands and tool handles that evaluates the stress on tissues and anatomical structures, and their association with traumatic disorders. Indeed, the perception of discomfort in human hands interacting with handles was related to the concentration of localized forces in [21]. Human contact forces have been measured using sensorized gloves for grasping objects [22] and during handshaking [23]. In [24], the hand-handle forces and distributed pressures were measured using a capacitive pressure-sensing mat wrapped around three different handles. Besides, authors divide the hand surface into five zones to study the localized pressure peaks and the contact force within each zone. Force distribution is very important also in robotic hands, since it can affect on the durability of the hand or the objects with which the hand has contact. More recently, contact pressure has been proposed as an evaluation metric for soft robotic grippers [25]. Sometimes, only contact area information is analysed, e.g. to categorise prehensile patterns [18], or to assess the realism of human-robot handshaking [26]. Most notably, in both these examples a simple technique was adopted, where either the hand or the object was painted and then paint-transfer patterns were used to describe the contact occurred.

III. ANALYSIS

The introduction of an articulate palm in a robotic hand increases the total number of degrees of freedom that the hand can use to accomplish its tasks. An instrument that quantifies this effect is the manipulability ellipsoid [27] of

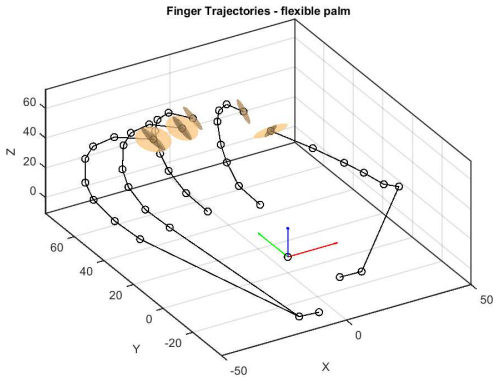

Figure 2. Comparison of manipulability ellipsoids between systems at 75% of closure. Translucent yellow ellipsoids correspond to the articulate palm, while black ellipsoids to the rigid palm. The kinematic chain of each finger and the palm planes is visible in black. Note that the index and middle fingers present the same ellipsoid as its base (palm plane) is fixed and equal in both conditions.

Table I
MANIPULABILITY: ELLIPSOIDS VOLUME & CONDITION NUMBER
F=FIXED, A=ARTICULATED

	Thumb	Index	Middle	Ring	Fifth
	Volume				
F	$1.24 \cdot 10^4$	$1.28 \cdot 10^4$	$1.28 \cdot 10^4$	$1.28 \cdot 10^4$	$1.28 \cdot 10^4$
A	$5.82 \cdot 10^4$	$1.28 \cdot 10^4$	$1.28 \cdot 10^4$	$6.80 \cdot 10^4$	$6.76 \cdot 10^4$
	Condition Number				
F	46.23	48.05	47.78	47.78	48.05
A	14.64	48.05	47.78	14.85	17.98

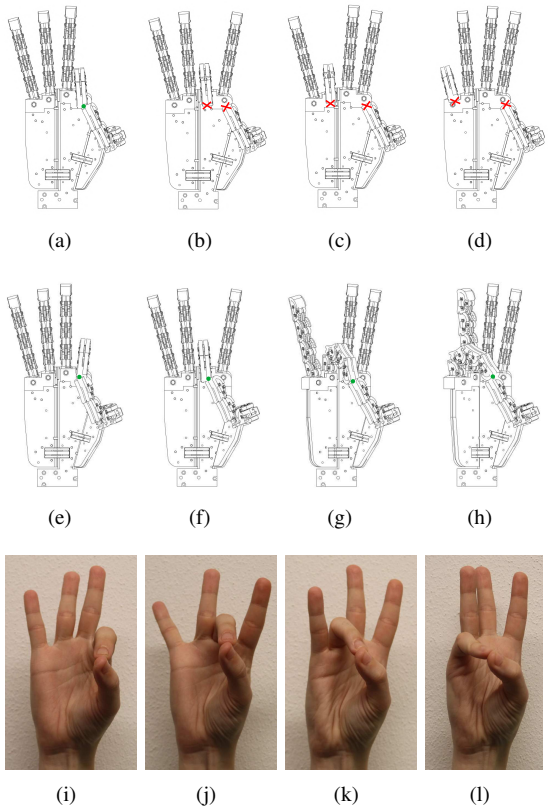

Figure 3. Kapandji test. Simulation of grasping capabilities of the fixed palm system (a-d), the modular palm (e-h) from a 3D CAD software and a human hand (i-l). A green dot indicates the success of the contact between fingertips, while a red cross is used to mark the opposite.

the fingertips. Considering a kinematic chain in a given configuration: the associated manipulability ellipsoid is defined as the set of all the end-effector velocities that the robot can locally achieve, assuming a limited amount of joint-level speeds that can be operated by the robot. It visualizes those directions in which the robot can move easily (where the ellipsoid has a larger radius), and those in which the robot moves with difficulty, or hardly at all (where the ellipsoid radius gets smaller). When the ellipsoid is round, the robot can move easily in all directions, while when the robot Jacobian matrix is close to a singularity, it becomes oblong.

To quantify the kinematic improvement derived from palm flexibility, we compare the Cartesian Manipulability Ellipsoids of a hand with an articulate palm, to those of a similar hand where the palm is fixed (see Fig. 2). The articulate palm can flex along two axes: one between the index and thumb, and another between the middle and ring fingers. This movement affects on the ellipsoids of the thumb, ring and fifth finger, that are larger for the articulate palm hand (translucent yellow) than for the fixed palm one (translucent black). Moreover, the fact that the black ellipsoids are more eccentric indicates that the fingers of the fixed palm hand have poor mobility in some directions. This is confirmed by a larger volume and a smaller condition number (see Table I) of the ellipsoids of the thumb, ring and fifth finger, both indicators of smaller eccentricity, thus a better manipulability. Contrarily, all long fingers have a very thin and oblong ellipsoid for the fixed palm hand, an indicator of closeness to motion singularity. This means that they tend to move along one direction only, which limits the hand possibility to execute a given task.

Manipulability ellipsoids rely on local measures of joint angles and Jacobians, and express a local description of fingers mobility. A complementary point of view is given by the Kapandji test [28], a clinical metric for the evaluation of the opposition of the thumb after a trauma or a surgery. It relies on the existence of a solution to the inverse kinematic problem of finding a contact between pairs of fingers.

To assess the kinematic improvement in terms of the possibility to have opposition between fingers, Fig. 3 compares the kinematics of two robotic hands, one whose palm is fixed and one whose palm is articulated, to that of a human hand. In agreement with the previous results coming from both anatomical insight and manipulability analysis, the system with a fixed palm configuration (0° for the hypothenar angle and 25° for the thenar angle) can only flex the thumb against the index (see Fig. 3(a)). This hand is able to perform pinch, as does the standard closure of most of robotic hands where the opposition is only embedded in the thumb joint. On the contrary, the hand with articulated palm allows the opposition of the thumb with each of the long fingers by relying on different configurations of the palm planes, as occurs in humans. Fig.s 3(g) and 3(h) clearly show the importance of hypothenar palm movement to allow the existence of these contacts, and how the phalanges of the fingers opposing the thumb are rotated towards it.

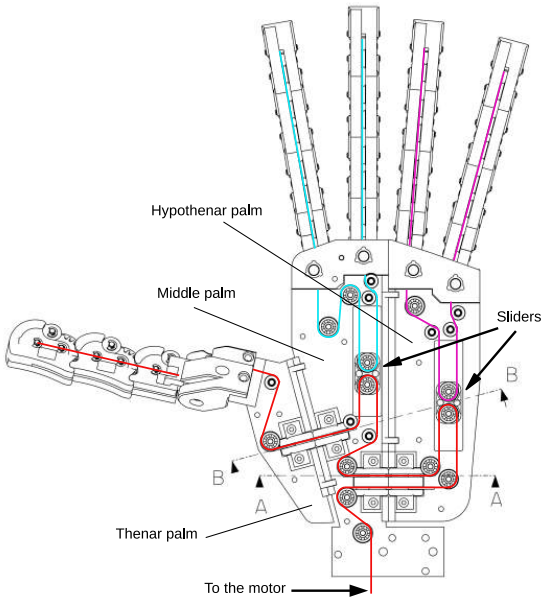

Figure 4. Mechanical design. The dorsal view of the palm design based on three planes movement and the routing required to define the under-actuation based on soft synergies concept.

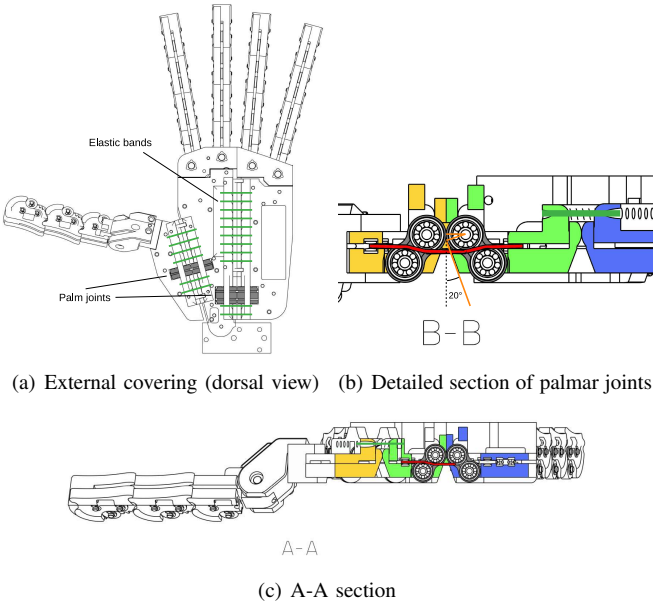

(a) External covering (dorsal view) (b) Detailed section of palmar joints

(c) A-A section

Figure 5. Mechanical design. Panel (a) shows the external side of the system, where elastic bands are placed to assure the rest position of the hand and its adaptability. Panel (b) presents a detailed description for palmar joints at B-B section with the maximum angle achievable from the contact point, and (c) shows the A-A section.

A good mobility of fingers is a fundamental component of grasping, because of the impact it has on the quantity and quality of the contact points that a hand can acquire. The pivotal role of contact points in grasp acquisition and control can be observed in the way humans plan digit placement [29] and in robots, where studies show that grasp stability depends, among other factors, on a good density and distribution of contacts [30]. Nevertheless, in under-actuated and adaptive grasping systems, finger motions are not fully specified by control. The hand-object system behaviour is determined by the equilibrium of motor actions, hand elasticity and reactions of the object [3]. This makes proving system capabilities when interacting with real objects fundamental. Therefore, to assess the effective improvement that larger manipulability of the fingertips will yield to a more adaptive robotic hand, we propose a design with the implementation of an articulated and flexible palm, for an existing under-actuated robotic hand. We aim at investigating how palm motions modify the hand capability of adapting to different shapes by measuring the effective contact area in grasping experiments, which is proportional to the number of contact points the hand is capable to achieve for a given object.

IV. DESIGN

The results of the previous analyses are applied to the design of a new version of the Pisa/IIT SoftHand [3], integrating an articulated and adaptive palm in its synergistic actuation layout, i.e. without additional motors. In particular, we decompose its palm in 3 modules able to articulate and form a concavity. As presented in Section III, this makes the thumb and the fifth and ring fingers to rotate towards the hand centre, increasing the quality of opposition of the thumb towards all other fingers.

Fig. 4 shows the mechanical design of the new system. An important feature of the new design is the inclusion of the palm actuation mechanism in the soft synergetic actuation scheme of the hand. This is obtained thanks to a particular routing of three tendons to actuate all the hand joints (see Fig. III). One tendon, red in Fig. III, routes from the motor through the three palm sections and two coupling sliders, up to the thumb. The other two tendons (cyan and purple) connect a pair of finger each to one of the coupling sliders. The choice of this cable routing design implements the same soft synergy than the previous version of the Pisa/IIT SoftHand, including in its adaptive under-actuation also the palm motions. Nevertheless, it yielded some constraints in our design freedom when deciding where to split the palm. Ultimately, the implemented thenar axis is at 77,31° with the base of the hand, while the hypothenar axis is at 90°. Although we did not have a reference hand kinematics to implement from literature, we recognize that such a thenar axis would be rather plausible to observe in humans, while the same can not be said for the hypothenar axis.

We used elastic bands on the dorsal part of the hand (see Fig. 5(a)) to implement the stiffness of the soft synergy and act as a return mechanism, similar to [3]. By tuning the resting length and stiffness of the bands, it is possible to adjust the resulting closure pattern. This tuning proceeded empirically until a behaviour compatible with the descriptions reported in [1] was observed. In the resultant motion, the thenar plane closes faster than the hypothenar plane. This configuration delays the hypothenar contribution to occur when the object is already in contact, favouring the adaptation of the hypothenar plane to the shape of the object. When we tried otherwise, we observed that the faster closure

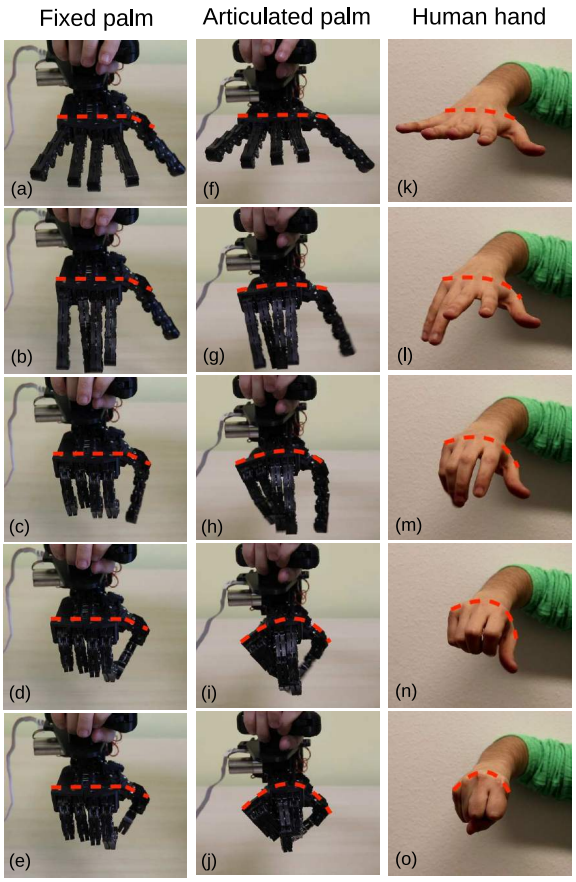

Figure 6. Palm concavity contribution in hands free-closure comparison. The dashed red lines represent the palm deformation.

of the hypothenar plane, and the consequent movement of the ring and fifth fingers, would push the object away from the centre of the hand, compromising its grasp.

The joints between the palm modules, presented in Fig. 5(c), are based on CORE joints. From the detailed view of the joint in section B-B (Fig. 5(b)), it is possible to observe a physical stop to limit the maximum joint angle to 40°. In the A-A and B-B sections, the routing of the tendon through the two bearings embedded in the joints is also visible.

Finally, Fig. 6 presents a sequence of pictures of the proposed prototype during a free-space closure, compared to the same design with a fixed palm, and a human hand. The fixed palm hand presents opposition mainly between the thumb and index fingers (Fig. 6(d)). This forces the objects to be grasped mainly in that area. On the articulated palm hand, all fingers converge in a more central position (see Fig.s 6(i) and 6(j)), allowing the grasp to occur in a location where a larger contribution of all the hand components is possible. As can be seen, the proposed palm allows for a more realistic power grasp closure, producing a concavity closer to the ones of human hands (Fig. 6(o)). This increases hand functionality, possible contact surface and grasp stability.

V. EXPERIMENTAL VALIDATION

In Section III we showed that the addition of two palmar DOFs increases the mobility of fingertips, yielding an improved adaptation potential of fingertips (testified by the higher manipulability) and a superior ability to oppose the thumb to the four long fingers (from the Kapandji test). Free motions of the implemented prototype (see Section IV) show how the inward rotations of the thenar and hypothenar planes make all fingers converge toward the hand centre, increasing the possible contribution of all fingers. All these behaviours, combined with the adaptive capability of the actuation system, suggest that the prototype should adapt better to the shape of different objects when grasping them. To assess adaptation capabilities and validate our hypothesis, inspired by literature discussed in Section II, we aim at quantifying the contact area achieved during the grasp action.

Note that, although grasp is a very complex phenomenon to describe mathematically [31], it narrows down to the hand restraining an object through a set of contact points where the hand and the object exchange forces. To maintain the grasp in the presence of an external force (from the sole gravity to any kind of external perturbations) there must be a feasible set of contact forces that can cancel out that force. Feasibility is the key, as that is subject to many constraints, which depend on the various capabilities of the hand and the characteristics of the contacts. When comparing two grasps, in the simplifying hypothesis that nothing else changes, a larger set of contact points gives more degrees of freedom to solve the grasp equations and is likely to increase (formally does not decrease) the probability of finding a feasible solution. Finally, while most grasp theory usually considers the set of contact points and the exchanged forces finite, the reality is that usually a continuous distribution of stress is exchanged through several contact area patches. Therefore, in this work we assume a larger contact area as an indicator of a better probability of a stable grasp.

Using the metric of contact area to assess grasp (and thus hand) quality, we compare our prototype with and without the adaptable palm, and with the human hand. Moreover, we report and discuss episodic examples of functional manipulation.

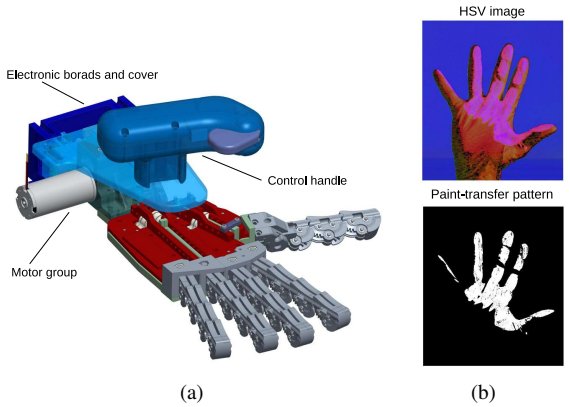

Figure 7. Panel (a) presents the experimental system, where the motor group and electronic boards are placed out of the palm movement. A mechanical handle with a sensorized trigger is used to control the closure of the synergy during the grasping experiments. Panel (b) shows an example of the two steps in the image processing.

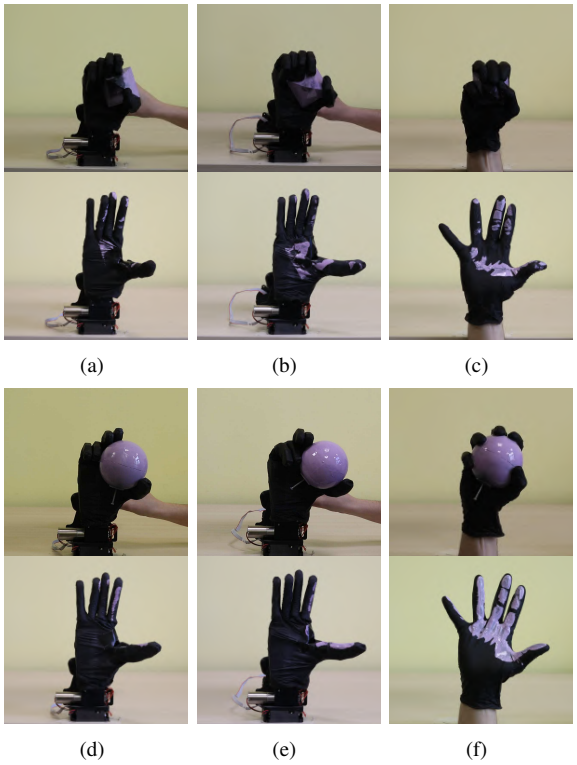

Figure 8. Example of contact area (paint-transfer patterns). Pyramid (a-c) and sphere (d-f). A comparison between the three hands studied is visible for each object in the following order: Fixed palm, adaptive palm and human hand.

Table II
PERCENTAGE OF PAINT IN HAND SURFACE

		Fixed	Adaptive	Human
Sphere	R=40mm	1.9%	4.8%	31.4%
Cube	edge=50mm	6.6%	7%	16.5%
Pyramid	edge=50; height=55mm	3.8%	10%	13.9%
Cylinder	d=20mm	1.5%	6.3%	21.9%
Cylinder	D=60mm	7.1%	6.5%	37%
Disk	d=80x23mm	11.9%	9.9%	21.8%

A. Materials and Methods

The experiment has the three hands (in a vertical position and with extended fingers pointing upward) grasping 6 objects of different shapes to elicit distinct grasping patterns. The specimens, a sphere, a cube, a pyramid, two cylinders and a disk, whose dimensions are detailed in Table II, were covered in wet paint to mark the contact points on the hand by direct transfer.

We executed the grasps with the prototype described in Section IV. The same prototype with the palm DOFs locked was used to analyse the behaviour of an identical robot hand with fixed palm angles, while performing the grasp of the same set of objects. Finally,we conducted the experiment with a human hand to give a target value to compare to, and an insight on how natural is the grasping of the robotic hands.

The three hands were covered with a black disposable latex glove, to protect the mechanism from the paint and to serve as a high contrast medium. The two robotic hands were placed on a table at a distance of 103,5 cm from a camera. The human hand was placed as close as possible to the position of the robotic one, at a focal distance of 10 cm w.r.t. the robot hand, which was compensated for during the image processing phase.

The one Degree of Actuation of the two robotic hands is controlled by one of the experimenters via a spring-loaded lever, whose position is read and used as a reference for the robotic hand, using the setup shown in Fig. 7(a). The hand motor is controlled with a PD control to the reference using a custom electronic board [32], which is also used for motor position sensing and for communication with a PC running Matlab/Simulink. Note that, for the same object, we did not compare grasps resulting from the same initial relative position between the hands and the object, since the choice of the relative position is a fundamental parameter determining the quality of the resulting grasp. Therefore, rather than opting for one common starting position, that would have favoured either one hand or another (or even disfavoured all of them), we opted for comparing the best performance of each hand on a given object. The optimization of the grasp was empirical. In particular, while one experimenter controlled the hand closure, another experimenter held the object in different positions until the hand performed a safe grasp. We chose to replicate the relative position between the object and the human hand as the starting point for the optimization and proceeded based on trial and error and on the experience of the authors. This is a limitation of this work, that should be fixed by optimizing the resulting grasp algorithmically. Unfortunately, a solution to this problem, which many authors would argue is not even unanimously reached yet, would have required a very good descriptive model of all the hands and the object, which is very difficult to obtain.

Finally, once the optimal configuration was found, we repeat the experiment with the object painted pink, to maximize contrast. Once a satisfactory grasp is recorded, the hand is opened back and a picture of the hand with transferred paint is acquired by the camera and processed with Matlab image processing toolbox.

We cropped the image to assure the processing of the hand surface exclusively. The pictures from the human hand were cropped with a larger window ($\sim 10\%$) to account for their different focal distance from the camera (10 cm). We resize all the pictures to have the same number of total pixels. The image colours were transformed from RGB to HSV, as in Fig. 7(b), top. Pixels within a threshold range of the paint colour were counted as containing paint. An example of this is visible in Fig. 7(b), bottom. The same process was done to extract the black pixels, that together with the pink ones, gave the amount to the total exposed surface of each hand. From these measures, the percentage of painted pixels over the total hand pixels was used as an estimate of the amount of contact area reached by the hand.

B. Results

The percentage of contact area for each of the examined cases is reported in Table II. Fig. 8 shows an example of

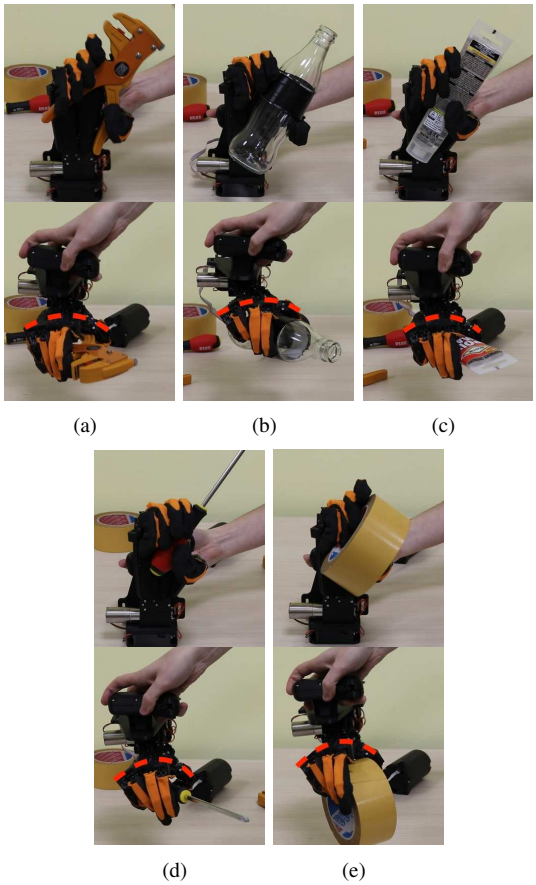

Figure 9. Grasping of five functional objects with the adaptive palm system. The top row shows a frontal grasp of the objects making contact in most of the fingers, while the bottom row highlights palm contribution with different concave deformation. The red dashed line represents the palm deformation.

the results collected with the three hands for two of the six objects. With respect to the compact and quantitative information reported in Table II, Fig. 8 highlights also the different distribution of the contacts. This figure shows also pictures shot during the grasp acquisition to give an idea of the object location and the grasping naturalness.

Additionally, Fig. 9 reports a group of pictures of more functional objects grasped with the adaptable palm. A brief attached video shows the free motion of the system closing, the adaptive under-actuation of the prototype when the palm is constrained, and some examples of the paint experiment and of the functional grasps.

VI. DISCUSSION

The contact percentage of the human hand is larger than both robotic systems in all conditions. Results with the human hand show that objects with a larger contact are the sphere and the cylinder (D=60 mm) with more than 30%, a significantly higher percentage compare to the one got with both robotic hands. Comparing the two robotic systems, the adaptable palm yields an improvement when grasping the sphere, the pyramid and the small cylinder (d=20 mm). Contrarily, the cube and the large cylinder (D=60 mm) obtained very similar scores. Finally, the disk, that elicits a palmar grasp, present better results for the system with a flat hypothenar angle, which is reasonable since the adaptable palm tends to oppose to remaining flat, exerting a force on the disk that tends to distance its flat surface.

Looking at the grasping pictures and the recorded videos, we realized that in many cases the robot hands tend to a grasp configuration that was more lateral compared to the human, because of the lower tendency the fingers have to oppose. A more lateral grasp forces the object to be positioned far from the centre of the palm and the rest of the fingers. Still, we observe a safer grasp with the adaptable hand, where more fingers tend to be involved in grasping, getting closer to a standard power grasp. The issue of having a different grasp can be seen also in the percentage values. For example in the sphere, where the object is far from the human position, we obtained a large difference among results. Instead, with the pyramid, where the object is close to the central position of the hand, the percentage of the adaptable hand is much closer to the human one, with 10% and 13%, respectively. These results suggest a further study on the design of the orientation of the hypothenar and thenar axis, which can be still forcing a lateral grasp compared to the natural one. Finally, in Fig. 9, where the adaptable palm hand is performing functional grasps on a group of common objects, the use of hypothenar and thenar palm adaptation is noticeable. Another important feature, also visible in Fig. 9, is that the palm angles are different in every condition, highlighting the capability of the hand to adapt to different shapes, favouring grasp safety, and suggesting the possible inadequacy of fixed palm angles to adapt to different objects.

VII. CONCLUSIONS

Human hands, in particular their palms, are described by an anterior and posterior surface that encompasses a hollow cavity that changes its shape during hand preshaping and grasping. Nonetheless, most of the robotic hands focuses on finger capabilities, while the palm contribution has been explored less often. To quantify the contribution of additional palmar DOFs in a robotic hand, we studied its effect on the fingertip manipulability, observing an improved kinematic adaptation potential, and an improvement in the capability of fingers to oppose each other.

Then, to investigate the contribution of an articulate palm to a soft under-actuated robot hand, we implemented this idea on the framework of the Pisa/IIT SoftHand, without introducing additional motors. We speculate that, thanks to the improved kinematics, the hand could acquire better grasps. To frame this hypothesis and be able to validate or disprove it, we narrow it down to obtain grasps with a larger contact area. The experiments we performed compared a soft robot hand with an adaptable palm to the same hand with a fixed palm and to a human hand. Results highlight an improvement of the contact area in 3 out of 6 cases, a substantial tie in 2 and a worse performance in only 1 case. Moreover, the adaptable palm yields better opposition of the fingers during grasping, which favours a more central position of the manipulandum. In particular, we observed a larger contribution of the hypothenar side of the palm and the

fifth and ring fingers to support the object. Finally, in more functional grasping examples, we observed the palm being modulated according to the shape of different objects, which seems to enlarge the design capabilities for adaptation. This wrapping capability could increase the contribution of all the hand components to the support of the object and therefore enhance grasp stability.

Although the experimental protocol is inspired by other literature [18],[26], the exclusive acquisition of contact area information, with no information about the contact forces, is an important limitation of our study. Indeed, the peak contact pressure is an important metric for the evaluation of the quality of the interaction. Therefore, in the future, we will consider adopting different experimental setups capable to assess the grasp quality also in terms of contact forces.

Another limitation of this study is in the choice of the orientation of hypothenar and thenar axis, which was heavily constrained by the implementation of the particular actuation scheme, and could be further investigated. Although our results are encouraging, complementary future studies could try to optimize several variables, e.g. human likeness, fingertip manipulability, or contact distribution during grasps.

Finally, we believe that the same concept could be investigated in prosthetics to study the reduction in cognitive load in more complex grasping conditions, the safety of grasping while holding and moving objects, and the comfort and acceptability of interaction.

ACKNOWLEDGMENTS

The authors warmly thank Vinicio Tincani and Cristiano Petrocelli for their valuable help in design support and manufacturing. Finally, Mattia Poggiani and Vinicio Tincani for helping in the execution of the grasping experiments.

REFERENCES

[1] A. P. Sangole and M. F. Levin, "Arches of the hand in reach to grasp," *Journal of biomechanics*, vol. 41, no. 4, pp. 829–837, 2008.

[2] ——, "A new perspective in the understanding of hand dysfunction following neurological injury," *Topics in stroke rehabilitation*, vol. 14, no. 3, pp. 80–94, 2007.

[3] M. G. Catalano, G. Grioli, E. Farnioli, A. Serio, C. Piazza, and A. Bicchi, "Adaptive synergies for the design and control of the pisa/iit softhand," *The International Journal of Robotics Research*, vol. 33, no. 5, pp. 768–782, 2014.

[4] O. J. Lewis, "Joint remodelling and the evolution of the human hand." *Journal of anatomy*, vol. 123, no. Pt 1, p. 157, 1977.

[5] C. Piazza, G. Grioli, M. Catalano, and A. Bicchi, "A century of robotic hands," *Annual Review of Control, Robotics, and Autonomous Systems*, vol. 2, pp. 1–32, 2019.

[6] H. Liu, K. Wu, P. Meusel, N. Seitz, G. Hirzinger, M. Jin, Y. Liu, S. Fan, T. Lan, and Z. Chen, "Multisensory five-finger dexterous hand: The dlr/hit hand ii," in *2008 IEEE/RSJ international conference on intelligent robots and systems*. IEEE, 2008, pp. 3692–3697.

[7] Z. Xu and E. Todorov, "Design of a highly biomimetic anthropomorphic robotic hand towards artificial limb regeneration," in *2016 IEEE International Conference on Robotics and Automation (ICRA)*. IEEE, 2016, pp. 3485–3492.

[8] R. Mahmoud, A. Ueno, and S. Tatsumi, "An interactive tele-operated anthropomorphic robot hand: Osaka city university hand," 2012.

[9] Elumotion, "Elumotion Ltd. website," http://elumotion.com, 2007.

[10] Shadow, "Shadow Robot Company website," https://www.shadowrobot.com, 2002.

[11] R. Deimel and O. Brock, "A novel type of compliant and underactuated robotic hand for dexterous grasping," *The International Journal of Robotics Research*, p. 0278364915592961, 2015.

[12] Y. Honda, F. Miyazaki, and A. Nishikawa, "Control of pneumatic five-fingered robot hand using antagonistic muscle ratio and antagonistic muscle activity," in *2010 3rd IEEE RAS & EMBS International Conference on Biomedical Robotics and Biomechatronics*. IEEE, 2010, pp. 337–342.

[13] I. A. Kapandji, *The Physiology of the Joints: Upper limb. v. 2. Lower limb. v. 3. The trunk and the vertebral column*. Churchill Livingstone, 1982.

[14] J. R. Napier, "The prehensile movements of the human hand," *The Journal of bone and joint surgery. British volume*, vol. 38, no. 4, pp. 902–913, 1956.

[15] H. Griffiths *et al.*, "Treatment of the injured workman." *Lancet*, pp. 729–33, 1943.

[16] R. J. Schwarz and C. Taylor, "The anatomy and mechanics of the human hand," *Artificial limbs*, vol. 2, no. 2, pp. 22–35, 1955.

[17] L. Sperling and C. Jacobson-Sollerman, "The grip pattern of the healthy hand during eating." *Scandinavian journal of rehabilitation medicine*, vol. 9, no. 3, pp. 115–121, 1977.

[18] N. Kamakura, M. Matsuo, H. Ishii, F. Mitsuboshi, and Y. Miura, "Patterns of static prehension in normal hands," *American Journal of Occupational Therapy*, vol. 34, no. 7, pp. 437–445, 1980.

[19] J. W. Nicholas, R. J. Corvese, C. Woolley, and T. J. Armstrong, "Quantification of hand grasp force using a pressure mapping system," *Work*, vol. 41, no. Supplement 1, pp. 605–612, 2012.

[20] C. Fransson and J. WINKEL, "Hand strength: the influence of grip span and grip type," *Ergonomics*, vol. 34, no. 7, pp. 881–892, 1991.

[21] R. Gurram, S. Rakheja, and G. Gouw, "A study of hand grip pressure distribution and emg of finger flexor muscles under dynamic loads," *Ergonomics*, vol. 38, no. 4, pp. 684–699, 1995.

[22] S. Shimizu, M. Shimojo, S. Sato, Y. Seki, A. Takahashi, Y. Inukai, and M. Yoshioka, "The relationship between human grip types and force distribution pattern in grasping," in *1997 8th International Conference on Advanced Robotics. Proceedings. ICAR'97*. IEEE, 1997, pp. 299–304.

[23] Z. Wang, J. Hoelldampf, and M. Buss, "Design and performance of a haptic data acquisition glove," in *Proceedings of the 10th Annual International Workshop on Presence*, 2007, pp. 349–357.

[24] Y. Aldien, D. Welcome, S. Rakheja, R. Dong, and P.-E. Boileau, "Contact pressure distribution at hand–handle interface: role of hand forces and handle size," *International Journal of Industrial Ergonomics*, vol. 35, no. 3, pp. 267–286, 2005.

[25] K. C. Galloway, K. P. Becker, B. Phillips, J. Kirby, S. Licht, D. Tchernov, R. J. Wood, and D. F. Gruber, "Soft robotic grippers for biological sampling on deep reefs," *Soft robotics*, vol. 3, no. 1, pp. 23–33, 2016.

[26] E. Knoop, M. Bächer, V. Wall, R. Deimel, O. Brock, and P. Beardsley, "Handshakiness: Benchmarking for human-robot hand interactions," in *2017 IEEE/RSJ International Conference on Intelligent Robots and Systems (IROS)*. IEEE, 2017, pp. 4982–4989.

[27] B. Siciliano, L. Sciavicco, L. Villani, and G. Oriolo, *Robotics: modelling, planning and control*. Springer Science & Business Media, 2010.

[28] A. Kapandji, "Clinical test of apposition and counter-apposition of the thumb," *Annales de chirurgie de la main: organe officiel des societes de chirurgie de la main*, vol. 5, no. 1, pp. 67–73, 1986.

[29] J. Lukos, C. Ansuini, and M. Santello, "Choice of contact points during multidigit grasping: effect of predictability of object center of mass location," *Journal of Neuroscience*, vol. 27, no. 14, pp. 3894–3903, 2007.

[30] C.-H. Xiong, Y.-F. Li, H. Ding, and Y.-L. Xiong, "On the dynamic stability of grasping," *The International Journal of Robotics Research*, vol. 18, no. 9, pp. 951–958, 1999.

[31] D. Prattichizzo and J. C. Trinkle, "Grasping," in *Springer handbook of robotics*. Springer, 2016, pp. 955–988.

[32] C. Della Santina, C. Piazza, G. M. Gasparri, M. Bonilla, M. G. Catalano, G. Grioli, M. Garabini, and A. Bicchi, "The quest for natural machine motion: An open platform to fast-prototyping articulated soft robots," *IEEE Robotics & Automation Magazine*, vol. 24, no. 1, pp. 48–56, 2017.